

## Evidence of ion diffusion at room temperature in microcrystals of the $\text{Bi}_2\text{Sr}_2\text{CaCu}_2\text{O}_{8+\delta}$ superconductor

M. Truccato<sup>a)</sup>

*"NIS" Centre of Excellence, Dipartimento Fisica Sperimentale, and INFN UdR Torino Università, Via Pietro Giuria 1, I-10125, Torino, Italy*

C. Lamberti and C. Prestipino

*"NIS" Centre of Excellence, Dipartimento Chimica I.F.M., and INFN UdR Torino Università, Via Pietro Giuria 7, I-10125, Torino, Italy*

A. Agostino

*"NIS" Centre of Excellence, Dipartimento Chimica and Generale ed Organica Applicata, INFN UdR Torino Università, C.so Massimo D'Azeglio 48, I-10125, Torino, Italy*

(Received 25 January 2005; accepted 28 April 2005; published online 20 May 2005)

We have studied Bi-2212 microcrystals aged at ambient conditions for 40 days. Combined x-ray absorption near edge structure and x-ray fluorescence measurements with micrometer space resolution show both an increase of  $\text{Cu}^+$  with respect to  $\text{Cu}^{2+}$  and an enrichment in Cu vs Bi and Sr cation content near the sample edges in the  $b$ -axis direction. A parallel study on an electrically contacted sample has indirectly detected the O loss, observing both a resistivity increase and an increase in sample thickness near the edges. We conclude that the O outdiffusion along the  $b$  axis is accompanied by Cu cation migration in the same direction. © 2005 American Institute of Physics. [DOI: 10.1063/1.1938251]

Single crystals of the  $\text{Bi}_2\text{Sr}_2\text{CaCu}_2\text{O}_{8+\delta}$  (Bi-2212) high- $T_c$  superconductor can be grown in samples whose length ( $\geq 500 \mu\text{m}$ ) is much greater than both their width and their thickness (whiskers). These kinds of samples have recently attracted remarkable interest from the point of view of both basic and applied physics. In fact, they have proved to be suitable systems for the study of the excess conductivity above  $T_c$  (Ref. 1) and of the transport properties along the  $c$  axis<sup>2</sup> because of their high quality and small sizes. Moreover, they are also good candidates for the fabrication of microscopic electronic devices based on the intrinsic Josephson junction stack structure.<sup>3</sup> Therefore, the check of the whisker homogeneity in terms of elemental and electronic structures has become an important issue. As far as bulk samples (i.e., with sizes greater than about  $1000 \times 200 \times 10 \mu\text{m}^3$ ) are concerned, it is well known that the material properties can be tuned by annealing in proper atmospheres. This procedure usually involves temperatures above  $400^\circ\text{C}$  in order to ensure homogeneous oxygen diffusion throughout the sample on a few hours time scale,<sup>4</sup> so that the O-diffusion length ( $\lambda$ ) is much greater than the sample size ( $\ell$ ). On the other hand, it has already been shown that Bi-2212 whiskers can undergo a significant increase in the in-plane resistivity when aged at room temperature on a two-year time scale,<sup>5</sup> most likely because of the oxygen loss induced by the favorable comparison between  $\ell$  and  $\lambda$ .

Variations in the O nonstoichiometry of Bi-2212 whiskers must be accompanied by a change of the Cu oxidation state in order to guarantee the electrostatic neutrality of the crystal. If  $\lambda$  is smaller or comparable with  $\ell$ , then a gradient in the O content, and therefore in the average Cu oxidation state, is expected. As  $\text{Cu}^+$  and  $\text{Cu}^{2+}$  have very different chemical behaviors, a significant local modification around

Cu cations is expected when they undergo the oxidation state variation. Due to its chemical selectivity, the x-ray absorption near edge structure (XANES) is the most suitable spectroscopic technique able to investigate both the oxidation and the coordination state of a selected transition metal cation inside a matrix.<sup>6-9</sup> As third generation synchrotron facilities provide microfocus beamlines, the determination of the local oxidation state of Cu inside aged Bi-2212 single crystals is possible at the micrometer scale. With this aim we have performed  $\mu$ -XANES experiments at the ID22 beamline of the ESRF synchrotron.<sup>10</sup> To verify whether the variation of the local Cu oxidation state, induced by O diffusion, is accompanied by a cation migration or not, x-ray fluorescence (XRF) has also been measured with the same spatial resolution of  $1 \mu\text{m}$  (vertical)  $\times 4 \mu\text{m}$  (horizontal).

In order to better appreciate the expected variation of the Cu oxidation state induced by O migration, samples were grown 40 days before the synchrotron measurements and aged at ambient conditions. The samples were prepared by the method of the oxygenation of melt quenched plates, resulting in crystals with typical dimensions of  $500 \times 20 \times 1 \mu\text{m}$  along the  $a$ ,  $b$ , and  $c$  axis, respectively. High-quality single crystals were selected at the optical microscope and either mounted on a glass capillary, for synchrotron measurements, or electrically contacted by Ag thermal evaporation and diffusion.<sup>5</sup> The single-phase character of the samples was checked by a standard four-probe measurement of the electrical resistance  $R$  vs the temperature  $T$ . The typical  $R(T)$  behavior is reported in the inset (a) of Fig. 1, which shows  $T_c = 79.1$  K. At the end of this experiment the sample was kept at room temperature for 12 h, then the  $R(T)$  measurement was repeated, resulting in the scattered triangles reported in inset (b) of Fig. 1. To appreciate the small but significant shift of the  $R(T)$  curve  $\Delta R/R \approx 5 \times 10^{-3}$  only a limited  $T$  interval has been reported, but the same  $\Delta R/R$  value holds over the whole measured  $T$  range. The observed

<sup>a)</sup>Electronic mail: truccato@to.infn.it

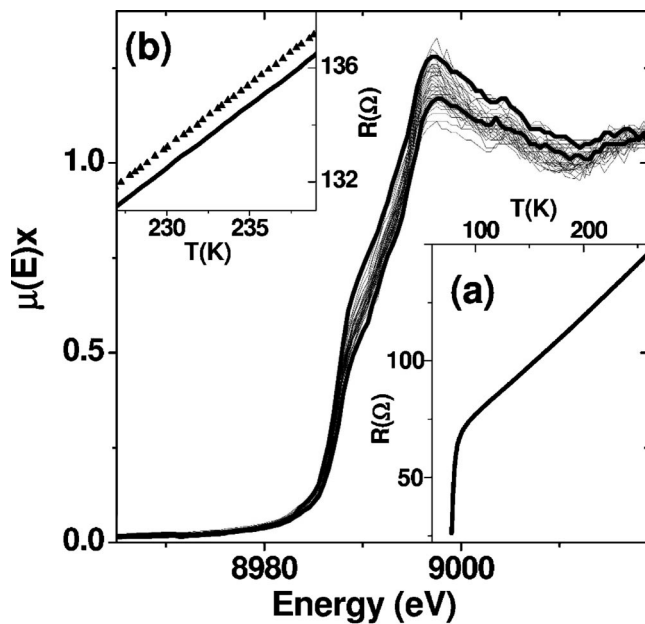


FIG. 1. Normalized XANES spectra collected on different positions of the Bi-2212 whisker. A shift of the edge up to 2.5 eV, accompanied by a modification of the white line intensity, clearly testifies an important modification of both the oxidation and the coordination state of Cu along the crystal. Bold curves represent spectra collected in central and in near-edge positions along the  $b$  direction, the others representing intermediate positions. Inset (a) reports the  $R$  vs  $T$  curve showing  $T_c=79.1$  K. Inset (b) compares, in a restricted  $T$  range, the original measurement (solid line) with its repetition after 12 h aging at 295 K (triangles).

increase of the resistance reflects the small, but indirectly measurable loss of O undergone by the sample during the aging at ambient conditions. By repeating the  $R(T)$  measurement on the sample aged 40 days, the observed  $\Delta R/R$  is  $\approx 30\%$ , reflecting a large electronic rearrangement to accommodate the anionic vacancies.

At the synchrotron the sample has been mounted on a goniometric head with the  $c$  axis parallel to the beam and the  $a$  axis forming an angle of  $4.95^\circ$  with respect to the vertical. The exact angle has been determined a posteriori from micro x-ray diffraction ( $\mu$ -XRD) data (see below). Owing to the huge difference in the crystal size along the  $a$  and  $b$  directions, the nonperfectly vertical geometry allowed us to finely scan the sample along the  $b$  direction by a simple vertical movement. Figure 1 reports the normalized XANES spectra, collected in fluorescence mode with a sampling step of 0.5 eV across the Cu  $K$  edge. The vertical scanning explores 90  $\mu\text{m}$  with a sampling step of 2  $\mu\text{m}$ . Doing so, the first spectrum is collected almost in the middle of the sample in the  $b$  direction and the last one is collected almost in the edge. By moving from the central position to the crystal edge, we observe an increase of the white line intensity (first resonance after the edge) of 10% and a redshift of the edge higher than 2 eV. This indicates an important gradient of the oxidation state of Cu along the  $b$  direction. At the crystal edges, where the atomic  $\text{O}^{2-}$  anions are supposed to recombine to give  $\text{O}_2$  molecules leaving the samples (and their four electrons), a significant  $\text{Cu}^+$  enrichment has been observed. As the energy shift between the  $K$  edge of pure  $\text{Cu}^+$  and  $\text{Cu}^{2+}$  model compounds is typically 5.0–6.5 eV (Refs. 6,7), assuming that in the central position of the crystal we still have a homogeneous population of  $\text{Cu}^{2+}$  cations, a fraction of about 30% of  $\text{Cu}^+$  is estimated at the edges. This experimental

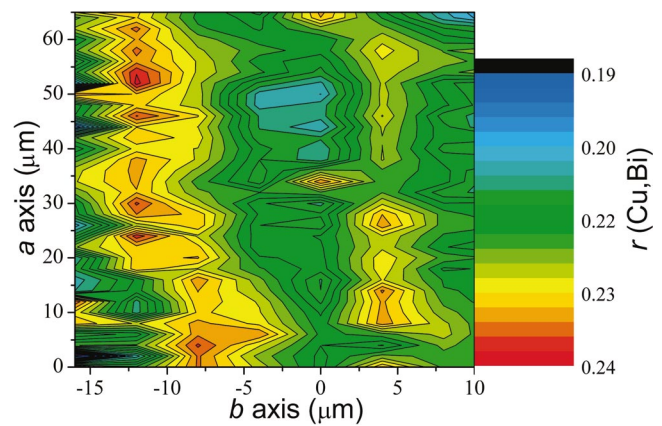


FIG. 2. (Color) Color scale XRF map reporting the  $r(\text{Cu,Bi}) = \text{Cu}(K_\alpha)/\text{Bi}(L_\beta)$  ratio on a portion of the same aged Bi-2212 sample used for the XANES study. The red regions correspond to the edge of the crystal. The axis labels (i.e.  $a$  and  $b$ -axis) just define the orientation of the crystal in the beam.

evidence suggests that in the O loss process the rate determining step is the  $\text{O}^{2-}$  migration to the crystal surface and not the  $\text{O}_2$  recombination at the surface. In this regard, Qui *et al.*<sup>9</sup> also have observed a variation of both edge position and white line intensity between the XANES spectra measured on an oxidized and on a reduced bulk Bi-2212 single crystal ( $1 \times 1 \times 0.1$  mm in size). However, the absence of a micrometer-focused beam forced the authors to collect the XANES spectra over the whole single crystal volume. As a consequence, the effects of the oxidation/reduction processes were averaged and the resulting differences in the XANES spectra were significantly smaller (0.5 eV of edge shift) with respect to what is observed here.

Finally, to verify whether the combined O migration and  $\text{Cu}^{2+}$  reduction has any effect on the local cation distribution, we have collected a 90- $\mu\text{m}$  (vertical)  $\times$  32- $\mu\text{m}$  (horizontal) two-dimensional XRF map by acquiring 2 s/point with a spatial sampling of 2  $\mu\text{m}$  (vertical)  $\times$  4  $\mu\text{m}$  (horizontal). We used a Li-doped Si detector perpendicular to the incident beam monochromatized at 17.3 KeV. The XRF resolution has been estimated to be better than 0.2 KeV from the full width at half maximum of the elastic peak, in agreement with the instrumental data sheet value of 160 eV. Together with the Compton signal (at 15.5 KeV) also the  $\text{Bi}(L_\alpha, L_\beta, L_\gamma)$  peaks, the Bi  $M$  multiplet, the  $\text{Sr}(K_\alpha, K_\beta)$  peaks, the  $\text{Cu}(K_\alpha, K_\beta)$  peaks and the  $\text{Ca}(K_\alpha, K_\beta)$  peaks have been detected. To avoid any systematic error related to the conversion of XRF counts into chemical stoichiometry, we decided to analyze the  $r(\text{Cu,Bi}) = \text{Cu}(K_\alpha)/\text{Bi}(L_\beta)$ ,  $r(\text{Cu,Sr}) = \text{Cu}(K_\alpha)/\text{Sr}(K_\alpha)$ , and  $r(\text{Bi,Sr}) = \text{Bi}(L_\beta)/\text{Sr}(K_\alpha)$  count ratios. By averaging these ratios in central and in lateral positions, the quantities  $\langle r_c(A,B) \rangle$  and  $\langle r_l(A,B) \rangle$  ( $A, B = \text{Cu, Bi, and Sr}$ ) were obtained, respectively. Being  $\langle r(A,B) \rangle$  the value of the ratio averaged over the whole map, the following three inhomogeneity factors  $f(A,B) = [\langle r_l(A,B) \rangle - \langle r_c(A,B) \rangle] / \langle r(A,B) \rangle$  ( $A, B = \text{Cu, Bi, and Sr}$ ) were obtained:  $f(\text{Cu,Bi}) = 0.10$ ,  $f(\text{Cu,Sr}) = 0.07$  and  $f(\text{Bi,Sr}) = -0.05$ . Figure 2 reports the  $r(\text{Cu,Bi})$  map over a fraction of the sampled region. From this figure the lateral Cu enrichment is apparent.

The whisker used for the electrical characterization was mapped by atomic force microscopy (AFM) at the end of the 40 days aging process and the result is shown in Fig. 3. The

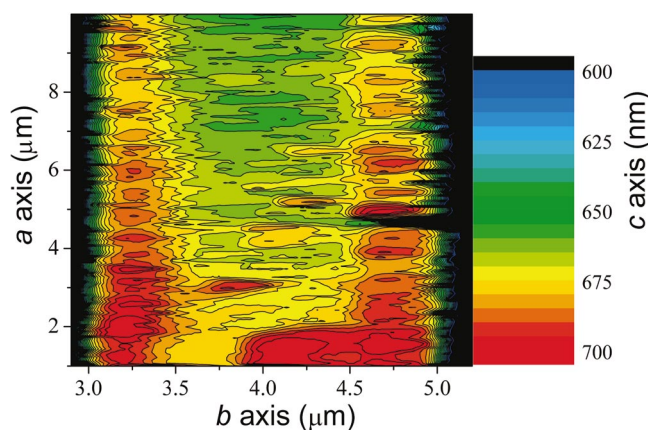


FIG. 3. (Color) Color scale AFM map of the Bi-2212 sample used for the electrical measurements at the end of the 40-day aging process. The red regions correspond to the edge of the crystal. The axis labels (i.e.  $a$ ,  $b$ , and  $c$ -axis) just define the crystal orientation.

crystal, exhibiting an almost flat  $a$ - $b$  surface in the as-grown condition, clearly shows an increased thickness  $\Delta z$  at the borders along the  $b$  direction. This is the consequence of the O depletion, which is known to induce an increase of the  $c$  axis lattice parameter<sup>11,12</sup> whose average over the crystal size along the  $c$ -axis direction ( $\approx 200$  unit cells) has been clearly detected by AFM. The  $c$ -axis increase, located at the border of the crystal along the  $b$  direction, well correlates with the higher fraction of  $\text{Cu}^+$  singled out in the same region by  $\mu$ -XANES (Fig. 1). These independent evidences agree well with the anisotropy in the in-plane O diffusion coefficients for Bi-2212 (Ref. 4) that testifies a slower migration process along the  $b$  direction and therefore enhances the possibility to evidence a compositional gradient. On a quantitative ground, the measured  $\Delta z/z$  (corresponding to  $\Delta c/c$ ) is  $\approx 4\%$ , indicating that the average  $c$  value on the  $b$  borders is around  $32 \text{ \AA}$ . Micro XRD measurements, collected in transmission mode with an image plate, resulted in a  $c$ -axis value of  $32.2 \text{ \AA}$  for the  $b$  border region.

Summarizing, we have presented a combined  $\mu$ -XANES and  $\mu$ -XRF study on a single crystal Bi-2212 sample. Space resolution, in the micrometer range, allowed us to single out a gradient along the  $b$  direction in the O content, evidenced by a change in the Cu oxidation state. Parallel AFM investigation has revealed a similar topological gradient in the  $c$  axis, which is again a consequence of the O gradient. It has turned out that these anionic, electronic, and structural rearrangements are accompanied by a cation migration producing a Cu enrichment at the border of the crystal.

We are indebted to R. Tucoulou and M. Drakopoulos for the technical support at ID22 beamline of the ESRF. We also thank N. Summa for her help in data analysis and the NIS Centre of Excellence for partial financial support.

<sup>1</sup>M. Truccato, G. Rinaudo, A. Causio, C. Paolini, P. Olivero, and A. Agostino, Phys. Rev. B (submitted).

<sup>2</sup>Y. I. Latyshev, T. Yamashita, L. N. Bulaevskii, M. J. Graf, A. V. Balatsky, and M. P. Maley, Phys. Rev. Lett. **82**, 5345 (1999).

<sup>3</sup>K. Inomata, T. Kawae, K. Nakajima, S. J. Kim, and T. Yamashita, Appl. Phys. Lett. **82**, 769 (2003), and references therein.

<sup>4</sup>T. W. Li, P. H. Kes, W. T. Fu, A. A. Menovsky, and J. J. M. Franse, Physica C **224**, 110 (1994).

<sup>5</sup>M. Truccato, G. Rinaudo, C. Manfredotti, A. Agostino, P. Benzi, P. Volpe, C. Paolini, and P. Olivero, Supercond. Sci. Technol. **15**, 1304 (2002).

<sup>6</sup>C. Lamberti, C. Prestipino, F. Bonino, L. Capello, S. Bordiga, G. Spoto, A. Zecchina, S. D. Moreno, B. Cremaschi, M. Garilli, A. Marsella, D. Carmello, S. Vidotto, and G. Leofanti, Angew. Chem., Int. Ed. **41**, 2341 (2002).

<sup>7</sup>C. Lamberti, S. Bordiga, F. Bonino, C. Prestipino, G. Berlier, L. Capello, F. D'Acapito, F. X. L. i Xamena, and A. Zecchina, Phys. Chem. Chem. Phys. **5**, 4502 (2003).

<sup>8</sup>R. Retoux, F. Studer, C. Michel, B. Raveau, A. Fontaine, and E. Dartyge, Phys. Rev. B **41**, 193 (1990).

<sup>9</sup>M. Qi, Z. F. Ren, Y. Gao, P. Lee, Y. L. Soo, and J. H. Wang, Physica C **192**, 55 (1992).

<sup>10</sup><http://www.esrf.fr/UsersAndScience/Experiments/Imaging/ID22/BeamlineManual>

<sup>11</sup>J. H. P. M. Emmen, S. K. J. Lenczowski, J. H. J. Dalderop, and V. A. M. Brabers, J. Cryst. Growth **118**, 477 (1992).

<sup>12</sup>B. Liang, C. T. Lin, A. Maljuk, and Y. Yan, Physica C **366**, 254 (2002).